Available online at www.sciencedirect.com
ScienceDirect
Journal of Organometallic Chemistry 691 (2006) 4289–4296
Journal of Organometallic Chemistry
www.elsevier.com/locate/jorganchem

Preparation and pyrolysis of poly(allyl iminoalane-*co*-ethyl iminoalane)s $[HAlN(allyl)]_m[HAlNEt]_n$

Yusuke Mori, Yasuhiro Kumakura, Yoshiyuki Sugahara *

Department of Applied Chemistry, School of Science and Engineering, Waseda University, Ohkubo-3-4-1, Shinjuku-ku, Tokyo 169-8555, Japan

Received 18 February 2006; received in revised form 27 June 2006; accepted 7 July 2006
Available online 14 July 2006

Abstract

Poly(allyl iminoalane-*co*-ethyl iminoalane)s {$[HAlN(allyl)]_m[HAlNEt]_n$; Allyl/Et-alanes}, have been prepared by reactions of lithium hydridoaluminate ($LiAlH_4$) with a mixture of allylamine hydrochloride ($CH_2{=}CHCH_2NH_2 \cdot HCl$; $allylNH_2 \cdot HCl$) and ethylamine hydrochloride ($CH_3CH_2NH_2 \cdot HCl$; $EtNH_2 \cdot HCl$) with various allyl/Et ratios. Spectroscopic analyses indicate that **Allyl/Et-alane(1/3)** (allyl/Et = 1/3) contains octamers possessing Al–H and C–H groups as well as C=C, Al–N, and C–N bonds. The loss of aluminum during pyrolysis of **Allyl/Et-alane(1/3)** at 1600 °C under an Ar atmosphere is 15%, which is less than the value reported for the pyrolysis of poly(ethyliminoalane) (36%). The suppression can be ascribed to cross-linking reactions involving allyl groups (hydroalumination and polymerization of the allyl groups), judging from infrared (IR) and solid-state nuclear magnetic resonance (NMR) spectroscopy.

Keywords: Precursor; Poly(allyl iminoalane-*co*-ethyl iminoalane)s; Pyrolysis; Hydroalumination; Aluminum nitride

1. Introduction

Pyrolytic conversion of precursors, which are typically organometallic and/or inorganic polymers possessing metal–nitrogen and/or metal–carbon backbones, is an established route to obtaining non-oxide ceramics and ceramics-based composites [1–5]. Desirable precursors should be fusible at relatively low temperatures or soluble in common organic solvents, since these properties are necessary for fabrications into ceramic materials with desirable shapes, including coatings and fibers. Precursors, moreover, should exhibit high ceramic yields in order to reduce shrinkage and cracks caused by gaseous species, which are generally hydrocarbons (or even gases containing metals), evolved during pyrolysis [1,3,5]. Since precursors with high ceramic yields generally possess highly cross-linked structures, however, the solubility is very low, which is a large drawback for the desired applications.

In order to prepare soluble precursors with relatively high ceramic yields, oligomers possessing reactive groups can be employed. Yive et al. reported that the cross-linking reactions (e.g. hydrosilylation) during pyrolysis of soluble oligovinylsilazane $[Si(CH_2{=}CH)(H)NH]_n$ led to a higher ceramic yield and a even lower loss of silicon (0.5%) in comparison with that for the pyrolysis of soluble oligomethylsilazane $[SiMe(H)NH]_n$ (46%) [6]. If the appropriate reactive groups (for example, Si–H, B–H, N–H and Al–H groups, or unsaturated organic groups) are introduced into precursors, therefore, cross-linking reactions before the volatilization can occur facilely, leading to exhibiting relatively high ceramic yields and suppressing the loss of the elemental components (in particular, metals) introduced into precursors drastically.

Poly(alkyliminoalane)s $[(HAlNR)_n$; PIAs] are well-known cage-type oligomers possessing an Al–N backbone, and their preparation procedures, structural characterization, various properties (such as reactivity and thermodynamic properties, etc.) and applications have been extensively investigated [7–9]. The pyrolytic conversion of PIAs into AlN has scarcely been reported, though

* Corresponding author. Tel./fax: +83 5286 3204.
E-mail address: ys6546@waseda.jp (Y. Sugahara).

0022-328X/$ - see front matter © 2006 Elsevier B.V. All rights reserved.
doi:10.1016/j.jorganchem.2006.07.004

numerous AlN precursors have been developed for past few decades [10–12]. We have prepared AlN from cage-type PIAs [13–16] and revealed the pyrolytic behavior at lower temperatures [17,18]. Although PIAs possess reactive Al–H groups, however, the loss of aluminum during pyrolysis of PIAs was relatively high because of the volatilization of low molecular mass species, including PIAs, at relatively low temperatures. The loss of aluminum during pyrolysis at 1600 °C was 36% [poly(ethyliminoalane), $(HAlNEt)_n$, n is mainly 8] and 55% [poly(isopropyliminoalane), $(HAlN^iPr)_n$, n is mainly 6] [14,15]. It is therefore expected that the loss of aluminum can be suppressed by designing the cage-type compounds via introduction of additional reactive groups.

Here we report the preparation of poly(allyl iminoalane-*co*-ethyl iminioalane)s {$[HAlN(allyl)]_m[HAlNEt]_n$; Allyl/Et-alanes}, from lithium hydridoaluminate ($LiAlH_4$), allylamine hydrochloride ($CH_2{=}CHCH_2NH_2 \cdot HCl$; allyl$NH_2 \cdot$ HCl) and ethylamine hydrochloride ($CH_3CH_2NH_2 \cdot HCl$; $EtNH_2 \cdot HCl$) with various allyl/Et ratios. The residues pyrolyzed at low temperatures (200–400 °C) are spectroscopically characterized to explore the pyrolytic behavior. We focus in particular on the reactions of the allyl groups ($CH_2{=}CH{-}CH_2{-}$) in the precursors at low temperatures, leading to suppressing the loss of aluminum. The characterization results of the residue pyrolyzed at 1600 °C are also presented.

2. Results and discussion

2.1. Spectroscopic characterizations of poly(allyl iminoalane-*co*-ethyl iminoalane)s

The IR spectra of the Allyl/Et-alanes, poly(ethyliminoalane) [$(HAlNEt)_n$, **Et-alane**] and poly(allyliminoalane) {$[HAlN(allyl)]_n$, **Allyl-alane**} are shown in Fig. 1. (The assignments are listed in Table 1.) The IR spectra of the Allyl/Et-alanes exhibit adsorption bands at 3078 cm^{-1} ($\nu_{CH_2=CH^-}$) [19], 3000–2760 cm^{-1} (ν_{CH}) [19], 1860–1820 cm^{-1} (ν_{AlH}) [7], 1635 cm^{-1} ($\nu_{C=C}$) [19], 1140–1080 cm^{-1} (ν_{CN}) [19] and ~720 cm^{-1} (ν_{AlN}) [20,21]. The appearance of these bands suggests the presence of Al–H and C–H groups as well as C=C, Al–N, and C–N bonds in the Allyl/Et-alanes. Since the IR spectra of all the Allyl/Et-alanes show similar profiles, only spectroscopic characterization of **Allyl/Et-alane(1/3)** (allyl/Et = 1/3) is represented below.

The ^{27}Al NMR spectra of **Allyl/Et-alane(1/3)** and **Et-alane** are shown in Fig. 2. The ^{27}Al NMR spectrum of **Allyl/Et-alane(1/3)**, as well as that of **Et-alane**, exhibits one broad signal at 135 ppm, which is assignable to the H*Al*N_3 environments [7,14,15,17].

The ^{13}C NMR spectra of **Allyl/Et-alane(1/3)** and **Et-alane** are shown in Fig. 3. (The assignments are listed in Table 2.) In the ^{13}C NMR spectrum of **Allyl/Et-alane(1/3)**, the resonances of the allyl group are observed at 141–135 ($CH_2{=}CHCH_2{-}N$), 120–114 ($CH_2{=}CHCH_2{-}N$) and 52–48 ($CH_2{=}CHCH_2{-}N$) ppm. The resonances of the ethyl groups are also observed at 45–38 ($CH_3CH_2{-}N$) and 23–18 ($CH_3CH_2{-}N$) ppm. The chemical shifts of the ethyl groups in **Allyl/Et-alane(1/3)** are similar to those in **Et-alane**.

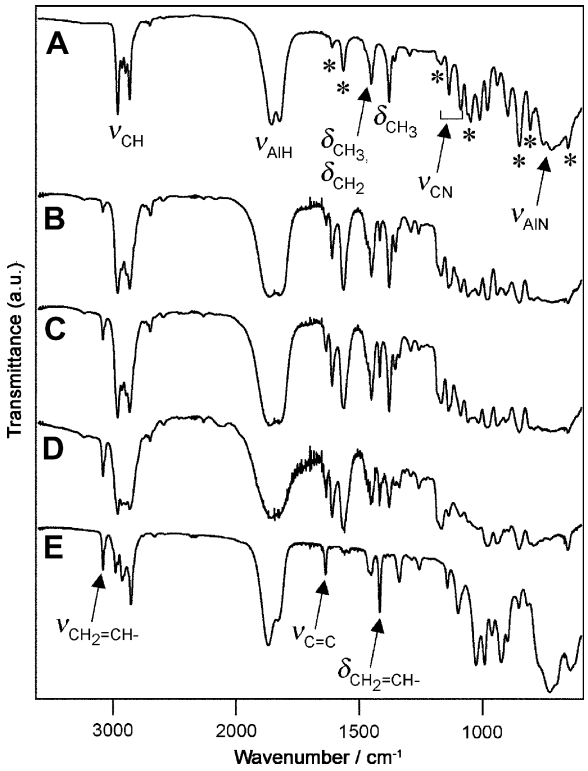

Fig. 1. IR spectra of: (A) **Et-alane**, (B) **Allyl/Et-alane(1/7)**, (C) **Allyl/Et-alane(1/3)**, (D) **Allyl/Et-alane(1/1)** and (E) **Allyl-alane**. The bands marked by asterisks are due to hexachloro-1,3-butadiene (hcb).

Table 1
The assignments of the adsorption bands in the IR spectra

Wavenumber/cm^{-1}	Assignment
3078	$\nu_{CH_2=CH^-}$
3000–2760	ν_{CH}
1860–1820	ν_{AlH}
1635	$\nu_{C=C}$
1470–1450	δ_{CH_2}, δ_{CH_3}
1420	$\delta_{CH_2=CH^-}$
1378	δ_{CH_3}
1140–1080	ν_{CN}
~720	ν_{AlN}

Allyl/Et-alane(1/3) was also characterized by mass spectroscopy and cryoscopy. In the mass spectrum of the precursor (as shown in Fig. 4), the ionization peaks at *m/e* 567, 579, 591 and 603 are assignable to $[(HAlNEt)_8\text{-}1]^+$, $\{[HAlN(allyl)][HAlNEt]_7\text{-}1\}^+$, $\{[HAlN(allyl)]_2[HAlNEt]_6\text{-}1\}^+$ and $\{[HAlN(allyl)]_3[HAlNEt]_5\text{-}1\}^+$, respectively (Table 3). The average relative molecular mass of the precursor determined by cryoscopy is 7.6×10^2. Based on these observations, we conclude that **Allyl/Et-alane(1/3)** contains mainly $[HAlN(allyl)]_m[HAlNEt]_n$ $(m + n = 8)$ oligomers, suggesting that essentially no cross-linking reactions, such

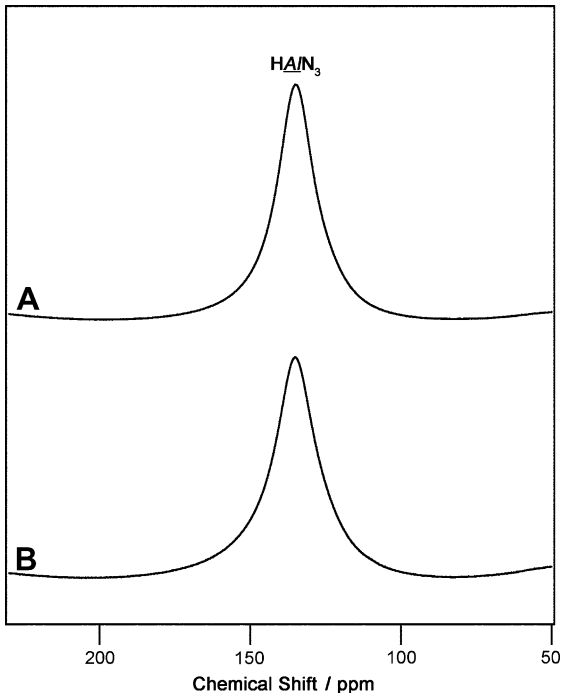

Fig. 2. ^{27}Al NMR spectra of (A) **Et-alane** and (B) **Allyl/Et-alane(1/3)**.

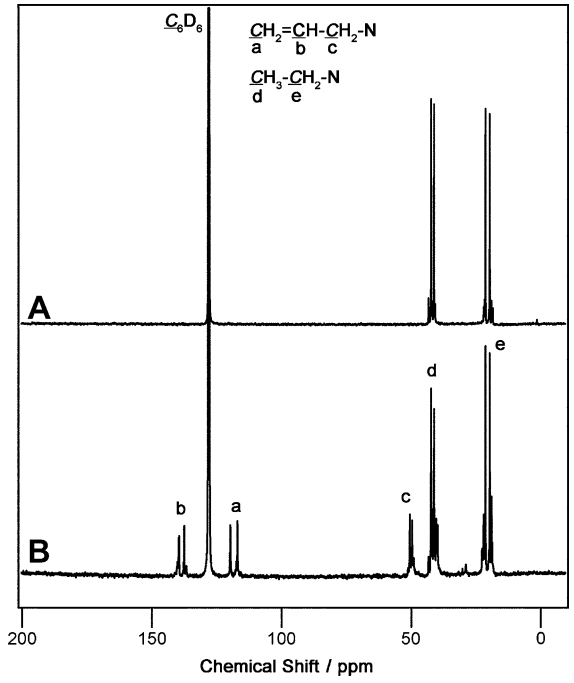

Fig. 3. ^{13}C NMR spectra of (A) **Et-alane** and (B) **Allyl/Et-alane(1/3)**.

Table 2
The assignments of the chemical shifts in the ^{13}C NMR spectra

Chemical shift/ppm	Assignment
141–135	CH_2=$CHCH_2$–N
120–114	CH_2=$CHCH_2$–N
52–48	CH_2=$CHCH_2$–N
45–38	CH_3CH_2–N
23–18	CH_3CH_2–N

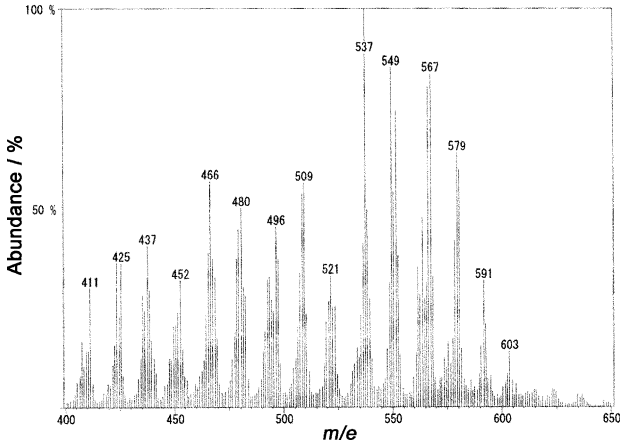

Fig. 4. Mass spectrum of **Allyl/Et-alane(1/3)**.

Table 3
Mass spectrum of **Allyl/Et-alane(1/3)** under electron ionization

m/e	Assignment	$[HAlN(allyl)]_m[HAlNEt]_n$
567	$[(HAlNEt)_8\text{-}1]^+$	$m = 0$, $n = 8$
579	$\{[HAlN(allyl)][HAlNEt]_7\text{-}1\}^+$	$m = 1$, $n = 7$
591	$\{[HAlN(allyl)]_2[HAlNEt]_6\text{-}1\}^+$	$m = 2$, $n = 6$
603	$\{[HAlN(allyl)]_3[HAlNEt]_5\text{-}1\}^+$	$m = 3$, $n = 5$

as hydroalumination and/or polymerization of the allyl groups, occur during the preparation of the precursor. No evidence for the occurrence of the cross-linking reactions is provided by the NMR results in accordance with the consideration of the molecular mass.

2.2. Conversion of precursors into ceramic residues

The TG curves of the Allyl/Et-alanes, **Allyl-alane**, and **Et-alane** are shown in Fig. 5. The ceramic yields of **Allyl/Et-alane(1/3)**, **Allyl/Et-alane(1/7)** (allyl/Et = 1/7), **Allyl/Et-alane(1/1)** (allyl/Et = 1/1), **Allyl-alane** and **Et-alane** up to

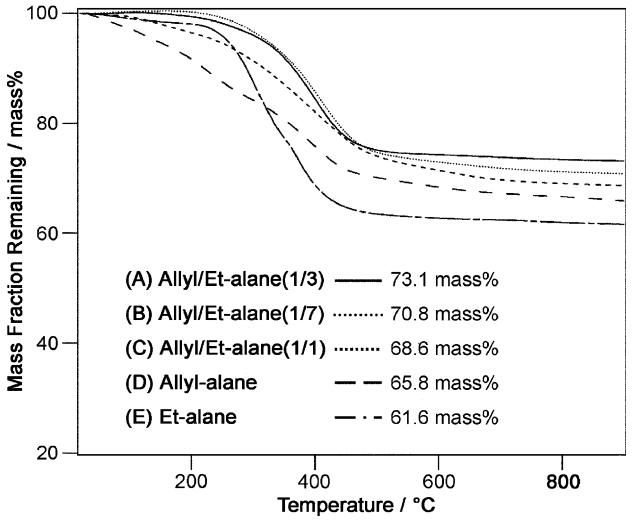

Fig. 5. TG curves of: (A) **Allyl/Et-alane(1/3)**, (B) **Allyl/Et-alane(1/7)**, (C) **Allyl/Et-alane(1/1)**, (D) **Allyl-alane** and (E) **Et-alane** under Ar flow.

900 °C are 73.1, 70.8, 68.6, 65.8 and 61.6 mass%, respectively. Thus, the ceramic yield of **Allyl/Et-alane(1/3)** is the highest among the precursors containing the allyl groups. Both **Allyl/Et-alane(1/3)** and **Et-alane** ($M = 568$) without the allyl groups [15] contain mainly octamers, but the ceramic yield of **Allyl/Et-alane(1/3)** is slightly higher than that of **Et-alane**. Since the mass loss cannot be observed above 500 °C, it is therefore assumed that the cross-linking reactions involving the allyl groups occur at low temperatures (below 500 °C).

Table 4 shows the compositions of **Allyl/Et-alane(1/3)** and the residue pyrolyzed at 1600 °C. The loss of aluminum during pyrolysis can be calculated by the following equation, based on the aluminum in the ceramic residue (C_{Al}), the aluminum in the precursor (P_{Al}) and the ceramic yield (Y).

$$\text{Loss(Al)}\ [\%] = [(P_{Al} - Y \times C_{Al})/P_{Al}] \times 100$$

The loss of aluminum [Loss(Al)] during pyrolysis of **Allyl/Et-alane(1/3)** is 15%, which is much smaller than that for the pyrolysis of **Et-alane** (36%) [15]. This observation suggests that the evolution of aluminum-containing species can be suppressed by the introduction of the allyl groups into the precursor.

2.3. Pyrolytic behavior of poly(allyl iminoalane-co-ethyl iminoalane)s at low temperatures

The IR spectra (not shown) of the residues pyrolyzed at 400 °C reveal that the $\nu_{CH_2=CH}$ band at 3078 cm^{-1} has vanished. Fig. 6 shows the IR spectrum of deuterated **Allyl/Et-alane(1/3)** $[DAlN(allyl)]_m[DAlNEt]_n$ (allyl/Et = 1/3) [hereafter abbreviated as ***d*-Allyl/Et-alane(1/3)**] pyrolyzed at 200 °C. The IR spectrum exhibits a ν_{CD} band at 2264 cm^{-1} [19].

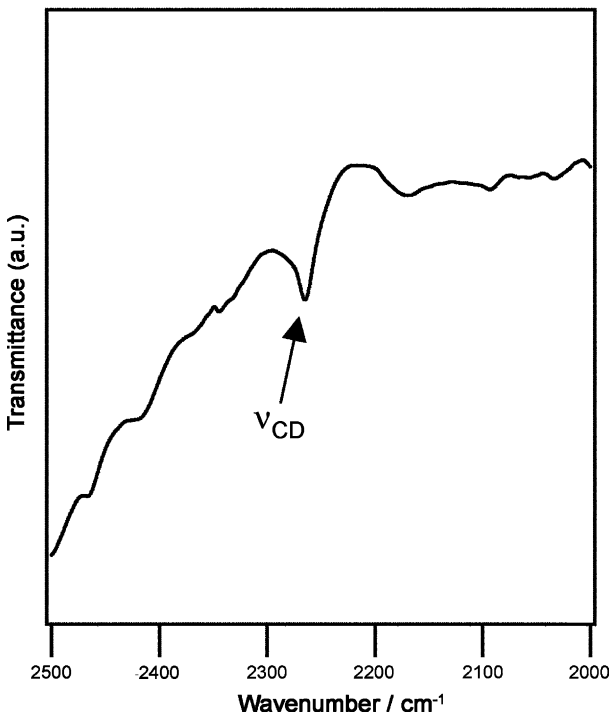

Fig. 6. IR spectra of ***d*-Allyl/Et-alane(1/3)** pyrolyzed at 200 °C.

Fig. 7 shows the solid-state ^{13}C NMR spectra of the pyrolyzed residues. (The assignments are listed in Table 5.) Two signals at 137 and 115 ppm, which can be assigned to the allyl groups, decrease gradually as the temperature increases in comparison with the signals assignable to the ethyl groups at 40 and 20 ppm. In addition, the solid-state ^{13}C NMR spectra exhibit two new signals. One signal at 10 ppm is assignable to the $CH_3C(sp^3)$ environment [22,23]. The other signal at 26 ppm is attributable to the $-CH_2C(sp^3)$ and/or $=CHC(sp^3)$ environments [22–24].

Fig. 8 shows the solid-state ^{27}Al NMR spectra of the pyrolyzed residues. (The assignments are listed in Table 6.) The spectra at 200–400 °C exhibit five signals at 111, 95, 70, 32 and 0 ppm and one shoulder at 130 ppm. The shoulder at 130 ppm and the signal at 111 ppm are attributable to the $HAlN_3$ [7] and AlN_4 environments [25], respectively. The signals at 32 and 0 ppm is assignable to the six-coordinated aluminum environment, because the resonances of the AlN_6 environment appear in the range between 6 and 45 ppm [26]. The signal at 70 ppm is tentatively assigned to the five-coordinated aluminum environment, because the resonances of the AlN_5 environment appear at ~83 ppm [26].

As for the assignment of the shoulder at 95 ppm, the broad signal of the $CAlN_3$ environment in $(EtAlNH)_n$ obtained by pyrolysis of $(Et_2AlNH_2)_3$ at 200 °C was observed at 100 ppm for the measurement at 14 T [27]. It is generally known that a smaller quadrupolar shift is observed by applying a higher magnetic field for ^{27}Al NMR [28]. Actually, the chemical shift of the AlN_4 environment is observed at 114–117 ppm (at 14 T) [29], 110 ppm (at 9.4 T) [25] and 103 ppm (at 4.7 T) [30]. For the signal assigned to the asymmetric $OAlN_3$ environment, the quadrupolar shift (106 ppm at 14 T [29], 93 ± 3 ppm at 9.4 T [31]) is also observed. Thus, the shoulder at 95 ppm measured at 9.4 T seems to be attributable to the $CAlN_3$ environment.

Table 4
The compositions of **Allyl/Et-alane(1/3)** and the residue pyrolyzed at 1600 °C

Sample	Elemental analysis/mass%						Compositional formula
	Al	N	C	H	O	Total	
Allyl/Et-alane(1/3)	36.0	18.6	36.0	7.7	–	98.3	$AlNC_{2.25}H_{5.74}$
Calculated [Allyl/Et-alane(1/3)]	36.4	18.9	36.5	8.2	–	100.0	$AlNC_{2.25}H_{6.00}$
1600 °C	49.2	22.8	22.7	–	4.5	99.2	$AlN_{0.89}C_{1.04}O_{0.15}$

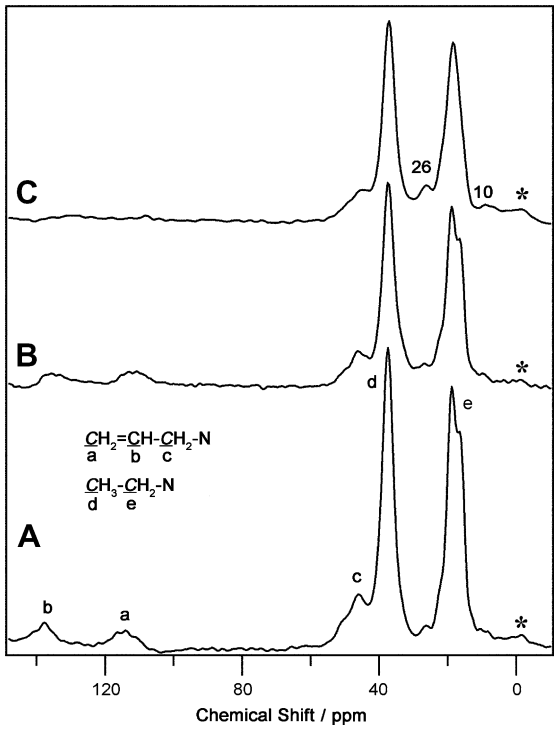

Fig. 7. Solid-state ^{13}C NMR spectra of **Allyl/Et-alane(1/3)** pyrolyzed at: (A) 200 °C, (B) 300 °C and (C) 400 °C. Spinning side bands are marked with asterisks.

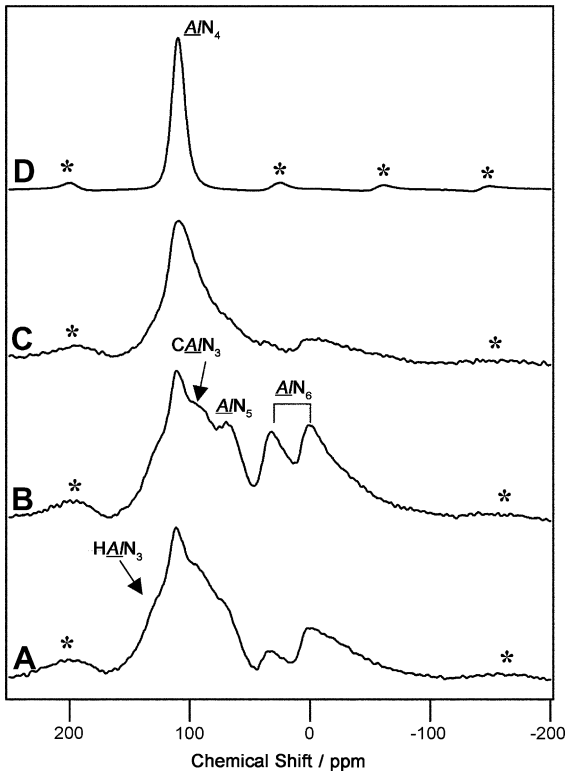

Fig. 8. Solid-state ^{27}Al NMR spectra of **Allyl/Et-alane(1/3)** pyrolyzed at: (A) 200 °C, (B) 300 °C, (C) 400 °C and (D) 1600 °C. Spinning side bands are marked with asterisks.

Table 5
The assignments of the chemical shifts in the solid-state ^{13}C NMR spectra

Chemical shift/ppm	Assignment
137	CH_2=*C*HCH_2–N
115	*C*H_2=CHCH_2–N
46	CH_2=CH*C*H_2–N
40	CH_3*C*H_2–N
26	–*C*H_2C(sp^3), =*C*HC(sp^3)
20	*C*$H_3$$CH_2$–N
10	*C*H_3C(sp^3)

Table 6
The assignments of the chemical shifts in the solid-state ^{27}Al NMR spectra

Chemical shift/ppm	Assignment
130	H*Al*N_3
111–110	*Al*N_4
95	C*Al*N_3
70	*Al*N_5 (tentative)
32, 0	*Al*N_6

In the temperature range from 200 to 400 °C, as indicated by the resonances and the bands assignable to the allyl groups in the results of the IR and solid-state ^{13}C NMR spectra, most of the allyl groups in **Allyl/Et-alane(1/3)** are reacted. Thus, it is expected that the cross-linking reactions involving the allyl groups, such as hydroalumination and/or polymerization of the allyl groups, could occur.

Hydroalumination forms new Al–C bonds from Al–H groups and C=C bond. If hydroalumination, which is a reaction between Al–D groups and C=C bond, occurs during pyrolysis of ***d*-Allyl/Et-alane(1/3)**, the formation of new C–D bonds is expected. Correspondingly, in the IR spectrum of the residue pyrolyzed of ***d*-Allyl/Et-alane(1/3)**, the ν_{CD} band at 2264 cm^{-1} is observed. In the solid-state ^{27}Al NMR spectra of the pyrolyzed residues of **Allyl/Et-alane(1/3)**, the shoulder assigned to the C*Al*N_3 environment is observed, indicating that the residues possess new Al–C bonds. In the solid-state ^{13}C NMR spectra, moreover, a signal assignable to the *C*H_3C(sp^3) environment [22,23] is observed at 10 ppm. The ^{13}C NMR spectra also exhibit the signal at 26 ppm, which is attributed to the –*C*H_2C(sp^3) and/or =*C*HC(sp^3) environments [22–24]. The formation of the *C*H_3C(sp^3) (10 ppm) and =*C*HC(sp^3) environments (26 ppm) is due to the α-addition on hydroalumination, while that of the –*C*H_2C(sp^3) environment (26 ppm) is due to the β-addition on hydroalumination. Based on these observations, it can be concluded that hydroalumination occurs to form new Al–C bonds during pyrolysis (Scheme 1a).

As far as polymerization of the allyl groups is concerned, this forms –CH(R)–CH_2–CH(R)–CH_2– [from head–tail (or tail–head) polymerization] and/or –CH_2–CH(R)–CH(R)–CH_2– [from head–head (or tail–tail) polymerization] linkages (R; CH_2–N≡). In the solid-state ^{13}C NMR spectra of the pyrolyzed residues, a signal centered at 26 ppm, which is assignable to the –*C*H_2C(sp^3) and/or =*C*HC(sp^3) environments [22–24], is observed. Although

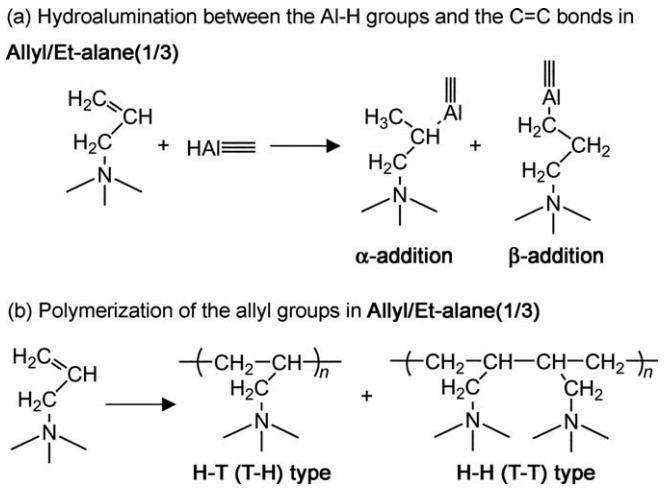

Scheme 1. Possible reactions during pyrolysis.

these environments can be formed via hydroalumination (as described above), they can also be obtained via polymerization of the allyl groups. We consequently could not exclude the possible polymerization of the allyl groups during pyrolysis (Scheme 1b).

The results of IR and solid-state NMR suggest that the allyl groups lead to the occurrence of the cross-linking reactions, involving hydroalumination and possibly polymerization of the allyl groups, during pyrolysis. It is consequently reasonable to assume that the cross-linking reactions make a significant contribution to the suppression of the loss of aluminum.

The Al–C bonds formed by hydroalumination and the C–C bonds formed by polymerization of the allyl groups should link the oligomers $\{[HAlN(allyl)]_m[HAlNEt]_n, (m+n=8)\}$. If these bonds are cleaved at the temperatures for the volatilization of low molecular mass species, such as the oligomers {the volatilization generally occur below ~300 °C in the case of the pyrolysis of **Et-alane** and poly(isopropyliminoalane) $[(HAlN^iPr)_n]$}, the volatilization of the oligomers should occur easily and, consequently, a considerable portion of aluminum in the precursors should be lost. It is therefore speculated that one possible reason for the suppression of the loss of aluminum is that the formed Al–C (and possibly C–C bonds) can survive at the temperatures for the volatilization of low molecular mass species at least partly.

2.4. Characterizations of the residue pyrolyzed at 1600 °C

The residue of **Allyl/Et-alane(1/3)** pyrolyzed at 1600 °C was characterized by solid-state ^{27}Al NMR, Raman, XRD and elemental analysis. As shown in Fig. 8, the solid-state ^{27}Al NMR spectrum of the residue exhibits one signal at 110 ppm, which can be assigned to the AlN_4 environment [25]. Fig. 9 shows the XRD pattern of the residue. The XRD pattern is consistent with that of crystalline AlN [32].

The residue was also analyzed with Raman spectroscopy (Fig. 10), which is one of the most sensitive methods for the

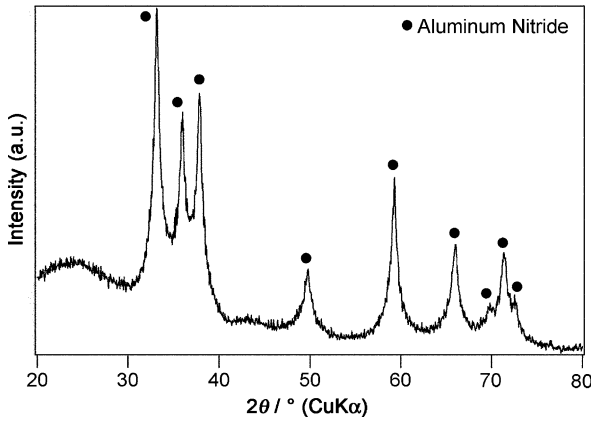

Fig. 9. XRD pattern of **Allyl/Et-alane(1/3)** pyrolyzed at 1600 °C.

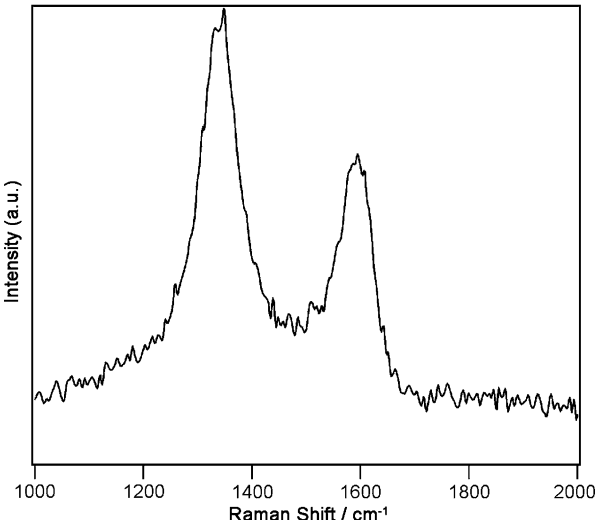

Fig. 10. Raman spectrum of **Allyl/Et-alane(1/3)** pyrolyzed at 1600 °C.

characterization of the various carbon phases [33–39]. The Raman spectrum of the residue exhibits two bands at 1337 and 1595 cm^{-1}, which are consistent with the Raman spectrum of amorphous carbon [40,41]. Based on these results, it is suggested that the pyrolyzed residue contains crystalline AlN and amorphous carbon.

The pyrolysis of precursors possessing both an Al–N backbone and Al–C bonds under an inert atmosphere led to the formation of AlN without any Al–C bonds [and aluminum carbide (Al_4C_3)] in the residues [12]. In this study, the result of the solid-state ^{27}Al NMR spectrum indicates that no Al–C bonds are present in the residue pyrolyzed at 1600 °C, indicating that the Al–C bonds formed by hydroalumination in the intermediates (i.e., the residue pyrolyzed at low temperatures) are cleaved during pyrolysis at high temperatures.

The ceramic yield of **Allyl/Et-alane(1/3)** up to 1600 °C is 62 mass%, which exceeds that of **Et-alane** (50 mass%) [15]. As shown in Table 4, a relatively high amount of carbon is present in the residue of **Allyl/Et-alane(1/3)** (22.7 mass%).

(The carbon in the residue of **Et-alane** is 17.1 mass% [15].) Based on these observations, it is assumed that the increase in the ceramic yield can be ascribed to both the suppression of the loss of aluminum and the increase in the carbon yield.

3. Experimental

All the manipulations were performed under a protective nitrogen atmosphere (purity: >99.9995%) using the standard Schlenk technique [42] or a nitrogen-filled glove box. Toluene (Kanto Chemical) was distilled over sodium and benzophenone under a nitrogen atmosphere.

3.1. Preparation of poly(allyl iminoalane-co-ethyl iminoalane)s

Poly(allyl iminoalane-*co*-ethyl iminoalane)s (Allyl/Et-alanes) were synthesized by reacting lithium hydridoaluminate (Wako Pure Chemical Industries) with allylamine hydrochloride (Tokyo Kasei Kogyo) and ethylamine hydrochloride (Tokyo Kasei Kogyo) as described below.

$$(m+n)\,\mathrm{LiAlH_4} + m\,\mathrm{allylNH_2\cdot HCl} + n\,\mathrm{EtNH_2\cdot HCl} \rightarrow [\mathrm{HAlN(allyl)}]_m[\mathrm{HAlNEt}]_n + (m+n)\,\mathrm{LiCl} + 3(m+n)\,\mathrm{H_2}$$

The ***d*-Allyl/Et-alane(1/3)** was also prepared from lithium deuteridoaluminate ($LiAlD_4$, Acros), allylamine hydrochloride and ethylamine hydrochloride.

The preparation of **Allyl/Et-alane(1/3)** is described below as a representative procedure, since the other precursors, **Allyl/Et-alane(1/7)** and **Allyl/Et-alane(1/1)**, were prepared in a similar manner. The reaction was conducted in a three-necked round-bottomed flask equipped with a gas inlet tube, a glass stopper and a reflux condenser. After it was carefully purged with nitrogen, the apparatus was charged with $LiAlH_4$ (9.259 g, 0.244 mol) and distilled toluene. Allylamine hydrochloride (5.707 g, 0.061 mol) and ethylamine hydrochloride (14.92 g, 0.183 mol) were then dried under reduced pressure for 3 h and added to this suspension. The mixed suspension was stirred overnight at 0 °C and then gradually heated to 110 °C. After stirring at 110 °C for 16 h, the product was filtered to remove insoluble components. Toluene was removed from the clear solution by trap-to-trap distillation under reduced pressure to yield a white solid.

For comparison with Allyl/Et-alanes, **Et-alane** and **Allyl-alane** were also prepared. **Et-alane** was synthesized by the methods reported previously [15]. **Allyl-alane** was obtained from $LiAlH_4$ and allylamine hydrochloride in the similar manner to the preparation of Allyl/Et-alanes.

3.2. Pyrolysis of poly(allyl iminoalane-co-ethyl iminoalane)s

For the pyrolysis at 200–400 °C, **Allyl/Et-alane(1/3)** was placed on a BN boat in a quartz tube under an argon atmosphere (purity: >99.999%) and pyrolyzed at 200, 300 and 400 °C with no holding time. The heating and cooling rate was 5 °C/min. For the pyrolysis at 1600 °C, **Allyl/Et-alane(1/3)** (1.2 g) was placed on a BN boat in an alumina tube under an argon atmosphere. The heating rate was 10 °C/min from room temperature to 200 °C and 5 °C/min from 200 to 1600 °C. The temperature was maintained at 1600 °C for 2 h, and the pyrolyzed residue was then cooled to room temperature at 5 °C/min (yield: 62 mass%).

3.3. Characterizations of poly(allyl iminoalane-co-ethyl iminoalane)s and the pyrolyzed residues

The Allyl/Et-alanes were characterized by infrared (IR) spectroscopy (JASCO, FT/IR-460), nuclear magnetic resonance (NMR) spectroscopy (JEOL, JNM-Lambda 500) and mass (MS) spectroscopy (JEOL, JMS-AUTOMASS). The IR spectra of the precursors were recorded using the hexachloro-1,3-butadiene (C_4Cl_6; hcb) technique. The ^{13}C NMR (125.65 MHz) spectra of the precursors were recorded as a benzene-d_6 solution using tetramethylsilane [$(CH_3)_4Si$, TMS, 0 ppm] as an external standard. The ^{27}Al NMR (130.20 MHz) spectra of the precursors were recorded on the same apparatus using $[Al(H_2O)_6]^{3+}$ (0 ppm) as an external standard. The mass spectra of the precursors were obtained by electron ionization in the range of 10–1000 amu. The ionization energy was 70 eV and the ionization temperature was 300 °C. The average masses of the precursors were measured by cryoscopy using distilled benzene. Thermogravimetry (TG, Perkin–Elmer, TGA-7) was carried out at a heating rate of 10 °C/min under flowing argon up to 900 °C.

The residues of **Allyl/Et-alane(1/3)** pyrolyzed at 200–400 °C were characterized by IR and solid-state NMR spectroscopy (JEOL, NM-GSX 400). The IR spectra of the pyrolyzed residues were recorded using the hcb technique. The solid-state ^{13}C NMR spectra of the pyrolyzed residues were obtained at 100.54 MHz (^{13}C) with cross polarization and magic angle spinning (CP/MAS) techniques. The solid-state ^{27}Al NMR (104.17 MHz) spectra were recorded with the MAS technique only. Five hundred scans were accumulated with a pulse delay of 5 s (^{13}C) or 1 s (^{27}Al) and a spinning rate of 7 kHz (^{13}C) or 9 kHz (^{27}Al). The residues pyrolyzed at 200–400 °C were packed in sample tubes in a nitrogen-filled glove box and kept under flowing nitrogen during the measurements.

The residue of **Allyl/Et-alane(1/3)** pyrolyzed at 1600 °C was characterized by solid-state ^{27}Al NMR spectroscopy, Raman spectroscopy (Thermo Electron, Nicolet Almega XR) and X-ray diffraction (XRD, Rigaku, Rint-2500) analysis. The solid-state ^{27}Al NMR spectrum of the residue was recorded on the same instrument employing the conditions described above. The X-ray diffraction pattern of the residue was obtained using monochromated Cu Kα radiation.

The amounts of aluminum in the precursors and the residue pyrolyzed at 1600 °C were determined using inductively coupled plasma (ICP) emission spectrometry

(Variant, Vista-MPX). The amounts of carbon, nitrogen and hydrogen in the precursor were determined with a Perkin–Elmer PE 2400-II instrument. The amounts of carbon, nitrogen and oxygen in the residue pyrolyzed at 1600 °C were determined with LECO CS-444LS and TC-436 instruments.

4. Conclusions

Poly(allyl iminoalane-*co*-ethyl iminoalane)s have been prepared through reactions between $LiAlH_4$, allylNH$_2$ · HCl and EtNH$_2$ · HCl with the allyl/Et ratios. All the Allyl/Et-alanes possess Al–H and C–H groups as well as C=C, Al–N, and C–N bonds, as revealed by the IR spectra. Spectroscopic analyses and cryoscopy indicate that **Allyl/Et-alane(1/3)** comprises oligomers, mainly the octamers $[HAlN(allyl)]_m[HAlNEt]_n$ ($m = 0$–3, $n = 8 - m$). During pyrolysis of **Allyl/Et-alane(1/3)** at 1600 °C, the loss of aluminum (15%) can be suppressed in comparison with that for the pyrolysis of **Et-alane** (36%). The suppression can be ascribed to hydroalumination and possibly polymerization of the allyl groups at low temperatures. These results suggest that the introduction of the allyl groups into oligomeric cage-type polyiminoalane is effective in suppressing the loss of aluminum, but simultaneously the amount of carbon, whose formation is not desirable, in the residue is also increased.

Acknowledgements

The authors gratefully thank Prof. Kazuyuki Kuroda, Department of Applied Chemistry at Waseda University, for valuable discussion. This work was supported by 21COE "Practical Nano-Chemistry" from MEXT, Japan.

References

[1] K.J. Wynne, R.W. Rice, Annu. Rev. Mater. Sci. 14 (1984) 297.
[2] G. Pouskouleli, Ceram. Int. 15 (1989) 213.
[3] C.K. Narula, Ceramic Precursor Technology and Its Applications, Marcel Dekker, New York, 1995.
[4] J. Bill, F. Aldinger, Adv. Mater. 7 (1995) 775.
[5] D. Seyferth, in: J.M. Zeigler, F.W. Gordon Fearon (Eds.), Silicon-Based Polymer Science: A Comprehensive Resource, Advanced in Chemistry Series, vol. 224, American Chemical Society, Washington, DC, 1990, p. 565.
[6] N.S.C.K. Yive, R.J.P. Corriu, D. Leclercq, P.H. Mutin, A. Vioux, Chem. Mater. 4 (1992) 141.
[7] M. Cesari, S. Cucinella, in: D.B. Sowerby, I. Haiduc (Eds.), The Chemistry of Inorganic Homo- and Heterocycles, Academic Press, London, 1987, p. 167.
[8] A.Y. Timoshkin, H.F. Schaefer III, Chem. Rec. 2 (2002) 319.
[9] A.Y. Timoshkin, Cood. Chem. Rev. 249 (2005) 2094.
[10] B.X. Liao, Y.K. Li, Y. Lu, J. Mater. Chem. 3 (1993) 117.
[11] G. Selvaduray, L. Sheet, Mater. Sci. Technol. 9 (1993) 463.
[12] Y. Mori, Y. Sugahara, J. Ceram. Soc. Jpn. 114 (2006) 461.
[13] Y. Sugahara, T. Onuma, O. Tanegashima, K. Kuroda, C. Kato, J. Ceram. Soc. Jpn. 100 (1992) 101.
[14] Y. Saito, S. Koyama, Y. Sugahara, K. Kuroda, J. Ceram. Soc. Jpn. 104 (1996) 143.
[15] S. Koyama, H. Takeda, Y. Saito, Y. Sugahara, K. Kuroda, J. Mater. Chem. 6 (1996) 1055.
[16] Y. Sugahara, S. Koyama, K. Kuroda, Key Eng. Mater. 159–160 (1999) 77.
[17] Y. Saito, Y. Sugahara, K. Kuroda, J. Am. Ceram. Soc. 83 (2000) 2436.
[18] S. Koyama, H. Takeda, T. Tsugoshi, K. Watari, Y. Sugahara, J. Ceram. Soc. Jpn. 114 (2006) 563.
[19] N.B. Colthup, L.H. Daly, S.E. Wiberley, Introduction to Infrared and Raman Spectroscopy, Academic Press, London, 1964.
[20] E.G. Brame Jr., J.L. Margrave, V.W. Meloche, J. Inorg. Nucl. Chem. 5 (1957) 48.
[21] J.F. Janik, E.N. Duesler, R.T. Paine, Inorg. Chem. 26 (1987) 4341.
[22] M. Weinmann, T.W. Kamphowe, P. Fischer, F. Aldinger, J. Organomet. Chem. 592 (1999) 115.
[23] M. Weinmann, T.W. Kamphowe, J. Schuhmacher, K. Müller, F. Aldinger, Chem. Mater. 12 (2000) 2112.
[24] H. Schumann, S. Dechert, S. Schutte, J.Y. Hyeon, M. Hummert, B.C. Wassermann, W. Kaminsky, A. Eisenhardt, K. Köhler, J. Eichhorn, Organometallics 22 (2003) 1391.
[25] N.D. Butler, R. Dupree, M.H. Lewis, J. Mater. Sci. Lett. 3 (1984) 469.
[26] J. Pinkas, T. Wang, R.A. Jacobson, J.G. Verkade, Inorg. Chem. 33 (1994) 4202.
[27] F.C. Sauls, W.J. Hurley Jr., L.V. Interrante, P.S. Marchetti, G.E. Maciel, Chem. Mater. 7 (1995) 1361.
[28] G. Engelhardt, D. Michel, High-Resolution Solid-State NMR of Silicates and Zeolites, Wiley, New York, 1987, p. 106.
[29] J.J. Fitzgerald, S.D. Kohl, G. Piedra, S.F. Dec, G.E. Maciel, Chem. Mater. 6 (1994) 1915.
[30] S. Hayashi, K. Hayamizu, O. Yamamoto, Bull. Chem. Soc. Jpn. 60 (1987) 761.
[31] M.E. Smith, J. Phys. Chem. 96 (1992) 1444.
[32] The JCPDS file: No. 25-1133.
[33] Y. Wang, D.C. Alsmeyer, R.L. McCreery, Chem. Mater. 2 (1990) 557.
[34] R.O. Dillon, J.A. Woollam, V. Katkanant, Phys. Rev. B 29 (1984) 3482.
[35] F. Tuinstra, J.L. Koenig, J. Chem. Phys. 53 (1970) 1126.
[36] R.J. Nemanich, S.A. Solin, Phys. Rev. B 20 (1979) 392.
[37] M.I. Nathan, J.E. Smith Jr., K.N. Tu, J. Appl. Phys. 45 (1974) 2370.
[38] M. Ramsteiner, J. Wagner, Appl. Phys. Lett. 51 (1987) 1355.
[39] L.C. Nistor, J. Van Landuyt, V.G. Ralchenko, T.V. Kononenko, E.D. Obraztsova, V.E. Strelnitsky, Appl. Phys. A 58 (1994) 137.
[40] S. Trassl, G. Motz, E. Rössler, G. Ziegler, J. Am. Ceram. Soc. 85 (2002) 239.
[41] G. Gregori, H.-J. Kleebe, H. Brequel, S. Enzo, G. Ziegler, J. Non-Cryst. Solids 351 (2005) 1393.
[42] D.F. Shriver, M.A. Drezdzon, The Manipulation of Air-Sensitive Compounds, second ed., Wiley–Interscience, New York, 1986.